Biointerface Research in Applied Chemistry
Open-Access Journal (ISSN: 2069-5837)

Article
Volume 13, Issue 4, 2023, 313
https://doi.org/10.33263/BRIAC134.313

Exploration of the Electronic, Spectroscopic Properties, and Bonding of an Antimalarial Drug of Chromium Arene–Quinoline Half Sandwich Complex in Aqueous Solution: A PCM Investigation

Reza Ghiasi [1,*], Maryam Rahimi [2]

[1] Department of Chemistry, East Tehran Branch, Islamic Azad University, Tehran, Iran; rezaghiasi1353@yahoo.com (R.G.);
[2] Department of Chemistry, Faculty of Science, Arak Branch, Islamic Azad University, Arak, Iran; m_rahimi12@yahoo.com (M.R.);
* Correspondence: rezaghiasi1353@yahoo.com (R.G.);

Scopus Author ID 6507495898
Received: 6.06.2022; Accepted: 6.07.2022; Published: 11.09.2022

Abstract: In this paper, using the mPW1PW91 functional, quantum chemical calculations were used to explore electronic, spectroscopic properties and bonding of an antimalarial drug of chromium arene–quinoline half sandwich complex in gas and aqueous phases. The solvent effects were examined using the self-consistent reaction field theory (SCRF) based on the polarizable continuum model (PCM). Reactivity parameters of the complex and chloroquine were compared. The molecular properties of these molecules were related to their biological activity. The studied complex and chloroquine's octanol-water partition coefficient (log P) were calculated and compared. The correlation between molecular hardness and biological activity was illustrated. The temperature dependence of thermodynamic parameters of the complex was investigated. Cr-C bonds in the studied drug were illustrated using NBO and QTAIM analyses.

Keywords: antimalarial drug; chromium arene–quinoline half sandwich complex; polarizable continuum model (PCM); NBO; QTAIM.

1. Introduction

Malaria rests very severe and difficult in great parts of the world and places a weighty social problem mainly on developing countries. Resistance to malaria parasites has been enhanced against various drugs [1, 2]. Experimental and computational investigations have been reported about the antimalarial activity of several molecules [3-13]. Various synthetic quinoline-based drugs have been provided to treat malaria. For example, chloroquine, mefloquine and amodiaquine are used [14]. Also, many investigations have revealed that organometallic complexes exhibit antimalarial activity.

The most effective metal-based antimalarial agents are chloroquine-based metallocenes of Ru(II) [15] and Fe(II)[16-18]. Ferroquine [17] is the most noticeable of these complexes. This complex is the primary organometallic antimalarial to go on to phase IIb clinical trials [19]. Also, complexes containing artemisinin, chloroquine, quinine, and mefloquine with metal ions such as Pd(II), Pt(II) [20], Au(I) [21], and Ga(III) [22] have been reported. Changing the antimalarial drug's structure by incorporating a redox-active, lipophilic metal center should

enhance membrane permeability and assist in the addition of the drug in the resistant parasite's food vacuoles, increasing its usefulness [23].

Organometallic analogs of chloroquine (CQ) are significant drug candidates that may overcome the extensive chloroquine resistance advanced by malaria parasites. For instance, the preparation and characterization of ferroquine have been reported [24]. The inclusive structure–activity relationship of ferroquine have been investigated, changing the site of the ferrocene unit and relating the drug candidate to analogous ruthenocene derivatives [15, 25-27]. In another study, preparations, characterizations, and antimalarial activity of two novel chromium arene: [η^6-*N*-(7-chloroquinolin-4-yl)-*N′*-(2-dimethylamino-methylbenzyl) ethane-1,2-diamine]tricarbonylchromium and [η^6-*N*-(7-chloroquinolin-4-yl)-*N′*-(2 dimethylaminobenzyl)-ethane-1,2-diamine]tricarbonylchromium have been reported [28].

Illustrations of the structure and electronic and spectroscopic properties of the various drugs have been reported in many pieces of research by computational investigations [29-34]. Also, nano-cages have reported computational studies about drug delivery [35-39].

In the present paper, we explored the electronic, spectroscopic properties and bonding of an antimalarial drug of chromium arene–quinoline half sandwich complex, [η^6-*N*-(7-chloroquinolin-4-yl)-*N′*-(2-diamino-methylbenzyl) ethane-1,2-diamine]tricarbonylchromium, by quantum-mechanics tools.

2. Materials and Methods

Gaussian 09 software package was used for optimization and vibrational analysis [40]. The standard 6-311G (d,p) basis set [41-44] was considered for all calculations. Considered functional was a one-parameter hybrid functional with adapted Perdew-Wang exchange and correlation (mPW1PW91) [45]. This function provides better consequences in the transition metal complexes than B3LYP [46-49].

The studied complex was considered in neutral and singlet states. The vibrational analysis confirmed the identities of the optimized structures as an energy minimum.

For studying the solvation effect, a self-consistent reaction field (SCRF) approach was used through the polarizable continuum model (PCM) [50].

The partition coefficient octanol/water (*c log P*) [51] was estimated by the following formula:

$$c\log P = \frac{\Delta G_{sol}^{aqua} - \Delta G_{sol}^{Octanol}}{2.303\ RT}$$

Natural bond orbital analysis [52] was performed at mPW1PW91/6-311G(d,p) level of theory using the NBO 3.1 program [53] implemented in the Gaussian 09 package.

Quantum theory of atoms in molecules (QTAIM) analyses were provided on the optimized geometries with the identical level of theory for optimization using the Multiwfn 3.7 software package [54, 55].

3. Results and Discussion

3.1. Energetic aspects.

The structure of the prepared antimalarial drug of chromium arene–quinoline half sandwich complex, [η^6-*N*-(7-chloroquinolin-4-yl)-*N′*-(2-dimethylamino-methylbenzyl) ethane-1,2 diamine]tricarbonylchromium and chloroquine molecule is presented in Figure 1.

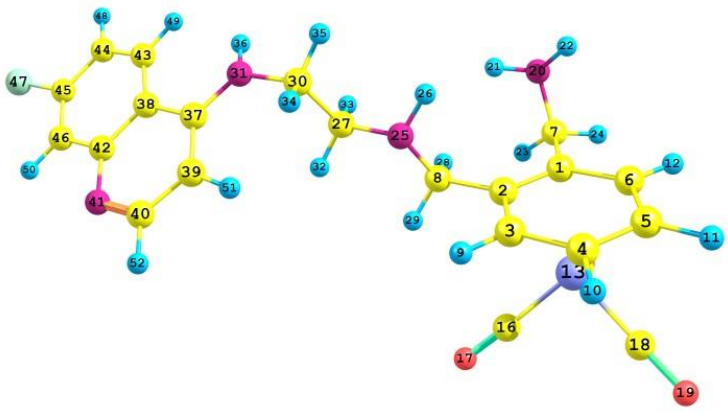

(a)

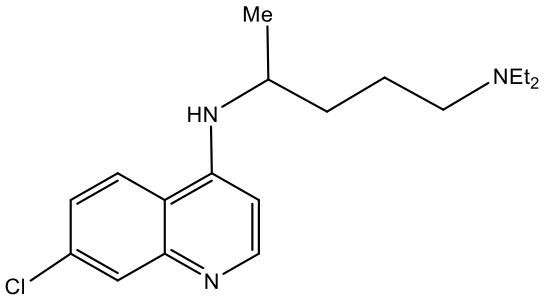

Chloroquine

(b)

Figure 1. Structures of (**a**) antimalarial drug of chromium arene–quinoline half sandwich complex and (**b**) chloroquine molecule.

We have replaced methyl substituents of amino groups of methylbenzene with hydrogen atoms to simplify the calculations. Therefore, we have carried out our calculations on the [η^6-*N*-(7-chloroquinolin-4-yl)-*N*′-(2-diamino methylbenzyl) ethane-1,2-diamine]tricarbonylchromium complex at the mPW1PW91/6-311G(d,p) level of theory in the gas phase and aqueous solution. The polarizable continuum model (PCM) is employed to assess the total energy of the studied structure in an aqueous solution. The studied complex's DFT-based computed total energy values are -2800.4689841 and -2800.4951294 a.u in the gas phase and in the aqueous solution, respectively. The DFT-based computed total energy values of the chloroquine molecule are -1326.072302 and -1326.0844995 a.u in the gas phase and in the aqueous solution, respectively. It can be observed that these drugs are more stable in an aqueous solution than in a gas phase. The aquation energy values of the studied complex and chloroquine molecule are -16.40 and -7.65 kcal/mol, respectively. Therefore, the title complex shows more stability in the aqueous phase than the chloroquine molecule.

3.2. Dipole moment.

Dipole moment is an important parameter to describe the biological characteristics specially attributed to the interaction with enzyme active sites of the molecules. The calculated dipole moment value of the title drug is 8.13 Debye in gas, indicating the polar nature of the studied drug. Hence, this complex with higher polarity is appropriate to bond metallically.

The calculated dipole moment of the studied complex is 12.39 Debye in an aqueous solution. The larger dipole moment value in the solution phase is found in the gas phase than

in the gas phase. A higher dipole moment value is attributed to long-range interactions of solvent with the solute molecules.

Calculated dipole moment values of the Chloroquine molecule are 6.16 and 8.42 Debye, in gas and aqueous phases, respectively. It can be found that the smaller values compared to the title complex.

3.3. Polarizability.

Mean polarizability <α> is calculated by the following equation [56]:

$$< \alpha >= \frac{\alpha_{xx} + \alpha_{yy} + \alpha_{zz}}{3}$$

Calculated α_{xx}, $\alpha_{yy,}$ and α_{zz} tensors values of the title drug are 426.60, 304.93, and 226.96 a.u. Therefore, the mean polarizability value is 319.50 a.u.

Polarizability value can be correlated to the hydrophobicity of a molecule and is usually considered a descriptor in QSAR studies [57].

The computed mean polarizability of the studied complex is 435.7 a.u in an aqueous solution. It can be seen that the larger <(> value in the solution phase is greater than in the gas phase.

Calculated isotropic polarizability values of the chloroquine molecule are 242.75 and 321.48 a.u, in gas and aqueous phases, respectively. It can be seen that these values are smaller than the title complex.

3.4. Molar refractivity.

Molar refractivity (MR) is a significant property in a quantitative structure-property relationship. It is directly correlated to the refractive index, molecular weight, and density of the steric bulk and is a factor for the lipophilicity and binding property of the studied system. The Lorentz-Lorentz equation is employed in the calculation of this parameter [58, 59]:

$$MR = \frac{n^2 - 1}{n^2 + 2} . \left(\frac{MW}{\rho}\right) = \frac{4}{3} . \pi . N . \alpha$$

where ρ is the density, n is the refractive index, MW is the molecular weight, (MW/ρ) is the molar volume, α is the polarizability of the molecular system, N is the Avogadro number, and its value depends only on the wavelength of light used to measure 'n'.

The value of MR for the studied drug is calculated as 119.39 and 90.71 esu for title complex and chloroquine molecule, which are responsible for the binding property of the complex and can be considered for the cure of various diseases.

3.5. Nonlinear optical properties.

The nonlinear optical effect is due to the interactions of electromagnetic fields in numerous media to yield novel fields altered in phase, frequency, amplitude, or other propagation characteristics from the incident fields. The first-order hyperpolarizabilities of the title complex and chloroquine molecule are 4.463×10^{-30} and 2.50×10^{-30} e.s.u., respectively. Here, the first hyperpolarizability of the title complex is 1.8 times that of the chloroquine molecule.

3.6. Frontier molecular orbital analysis.

The highest occupied molecular orbital energy (HOMO) and lowest unoccupied molecular orbital (LUMO) is played roles in chemical stability [60].

Figure 2 presents plots of frontier orbitals in the studied drug. It can be observed that the most significant contributions of atomic orbitals in the HOMO and LUMO are arisen from tricarbonylchromium and chloroquinolin fragments, respectively.

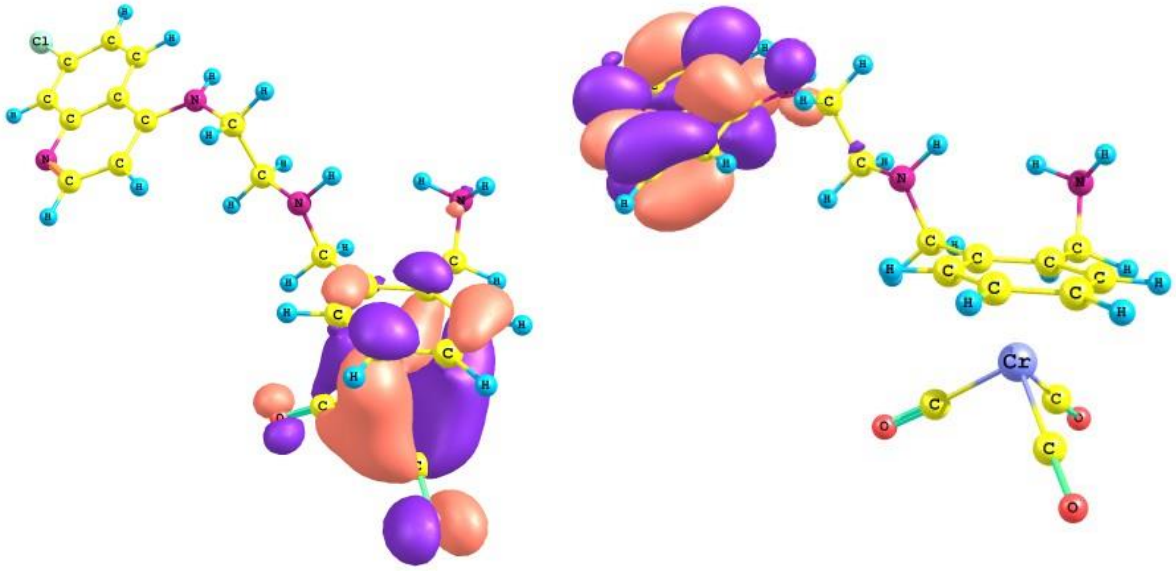

Figure 2. Plots of frontier orbitals in the studied chromium arene–quinoline half sandwich drug.

The HOMO-LUMO energy gap (ΔE = E(LUMO) – E(HOMO)) is an important stability index and also determines the electron transport properties. This parameter characterizes the kinetic stability and chemical reactivity of the molecule.

Soft systems are large and highly polarizable, while hard systems are relatively small and much less polarizable.

Frontier orbital energy and HOMO-LUMO gap values of this complex and chloroquine molecule are calculated in gas and aqueous phases (Table 1). It can be seen a larger HOMO-LUMO gap in the complex than in the chloroquine molecule. It can be seen a smaller HOMO-LUMO gap in the aqueous phase than in the gas phase.

Table 1. Frontier orbital energy, HOMO-LUMO gap, hardness (η), chemical potential (μ), and electrophilicity (ω) values (in eV) of the studied complex and chloroquine molecule in gas and aqueous phases at mPW1PW91/6-311G(d,p) level of theory.

	E(HOMO)	E(LUMO)	Gap	η	μ	ω
Complex						
Gas	-6.16	-1.43	4.72	2.36	-3.79	3.05
water	-6.06	-1.43	4.63	2.31	-3.75	3.04
Chloroquine						
Gas	-5.85	-1.28	4.57	2.28	-3.56	2.78
water	-5.75	-1.41	4.34	2.17	-3.58	2.96

On the other hand, E(HOMO) value reveals less stability of the HOMO in the solution phase than in the gas phase. In the solvent, polar solvents could indeed impact the geometry through long-range interactions with the solute molecules, stabilizing their frontier molecular orbitals. There are insignificant changes in E(LUMO) in solution and gas phases.

Global reactivity descriptors hardness (η), chemical potential (μ), and electrophilicity (ω) parameters help us to characterize the nature and interaction of the molecule [61-64]. It can be noticed that the values of global reactivity descriptors, the hardness, and the electrophilicity values of the complex decrease in going from the gas phase to the aqueous medium (Table 1). But, the complex's potential chemical value increases from the gas phase to the aqueous medium.

3.7. Structural parameters.

Calculated Cr-C and Cr-CO mean bond distances in the title drug are 2.194 and 1.837 Å, respectively, in the gas phase. Calculated Cr-C and Cr-CO mean bond distances in the title drug are 2.211 and 1.823 Å, respectively, in the aqueous phase. It can be found that Cr-C bond distances increase in the aqueous phase. But, Cr-CO bond distances decrease in the aqueous phase. Little alterations in the molecular structure may influence the biological activities of the drugs.

3.8. Vibrational assignments.

The total number of atoms, N, in the title anti-malaria drug is 52. Therefore, this complex has 150 (3N-6) normal vibrations modes.

The optimized geometry shows no special symmetry, so the complex fits the C_1 point group. The computed IR spectrum of the molecule is presented in Figure 3.

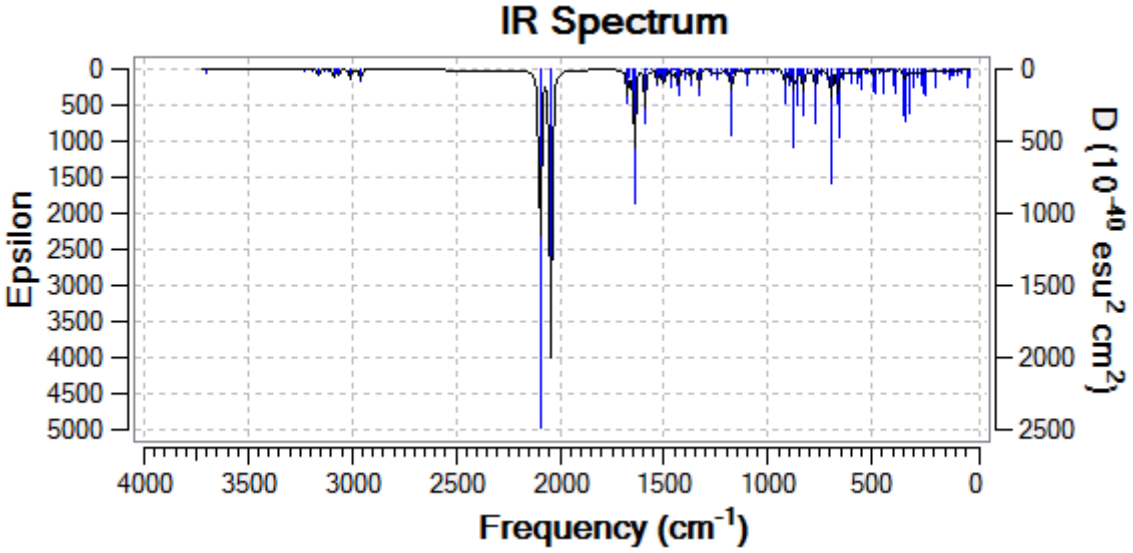

Figure 3. Computed IR spectrum of the studied chromium arene–quinoline half sandwich complex.

It can be observed the most intense bands are placed at 2040.21, 2046.70, and 2096.06 cm^{-1} in the gas phase. These vibrations are at 1965.68, 1969.09, and 2046.90 cm^{-1} in the aqueous phase. The vibration modes of these bands are shown in Figure 4. It can be found that these bands belong to symmetric and asymmetric stretching vibrations of CO ligands. It can be seen that the calculated wavenumber values decrease in the aqueous phase in comparison to the gas phase.

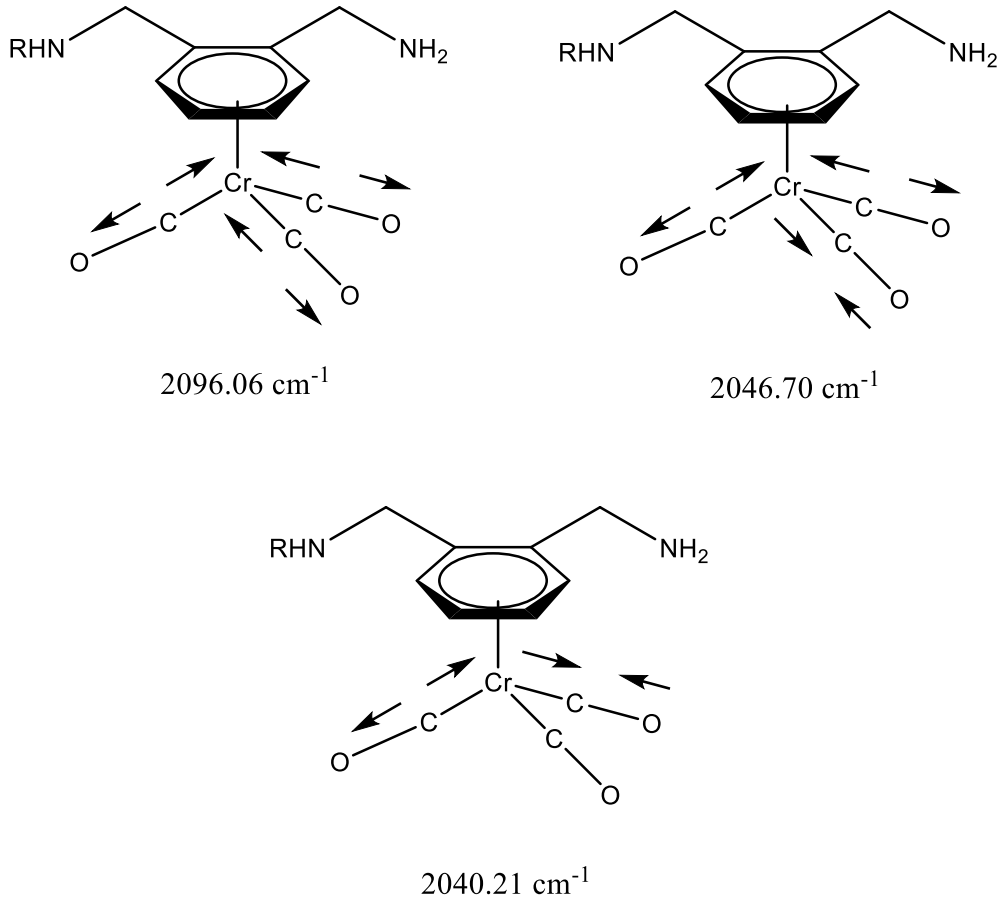

Figure 4. Vibration modes of the IR-active most intensity bands of the studied chromium arene–quinoline half sandwich complex.

3.9. Thermodynamical analysis.

The values of some thermodynamic parameters of studied chromium arene–quinoline half sandwich complex by mPW1PW91/6-311G(d,p) level are gathered in Table 2 (at 298.150 K and 1.00 atm). It can be deduced that the greater thermodynamic functions in higher temperatures ranging from 100 to 1000 K. can be attributed to the increasing molecular vibrational intensities in higher temperatures [65]. These calculated thermodynamics provide useful data for the additional investigation on the title drug. The correlation equations between heat capacity ($C^0_{p;m}$), entropy (S^0_m), enthalpy (H^0_m) changes, and temperature are:

$C^0_{p;m} = 0.2074\ T + 46.489;$ $R^2 = 0.9574$

$C^0_{p;m} = -0.0002\ T^2 + 0.397\ T + 8.5849;$ $R^2 = 0.9997$

$S^0_m = 0.3264\ T + 102.8;$ $R^2 = 0.9922$

$S^0_m = -0.0001\ T^2 + 0.452\ T + 77.669;$ $R^2 = 1.00$

$H^0_m = 0.0003\ T - 2800.1;$ $R^2 = 0.9761$

$H^0_m = 2\times10^{-7}\ T^2 + 9 \times 10^{-5}\ T - 2800.1;$ $R^2 = 0.9995$

Table 2. The standard statistical thermodynamic functions: heat capacity ($C^0_{p;m}$), entropy (S^0_m and enthalpy changes H^0_m for the title complex in various temperatures ranging from 100 to 1000 K at mPW1PW91/6-311G(d,p) level of theory.

T (K)	$C^0_{p;m}$	S^0_m	H^0_m
100	47.02	120.50	-2800.06

T (K)	$C^0_{p;m}$	S^0_m	H^0_m
200	79.72	164.49	-2800.05
300	111.80	203.73	-2800.03
400	140.92	240.55	-2800.01
500	165.37	275.16	-2799.99
600	185.20	307.49	-2799.96
700	201.27	337.59	-2799.93
800	214.45	365.62	-2799.90
900	225.41	391.77	-2799.86
1000	234.65	416.22	-2799.82

It can be seen that quadratic formulas fit correlations between the calculated thermodynamic parameters and temperature.

3.10. Partition coefficient.

Lipophilicity is one of the key properties used to investigate the important interactions between a drug and its biological receptor, which is regularly valued by means of the logarithm of the partition coefficient (log P). The larger the log P value, the more analgesic activity and lipophilic characteristics. Log P values of the complex and chloroquine are equal to -4.04 and -1.95. As observed, the log P value of the complex is less than chloroquine.

The biological activities of many compounds are related to hardness. Molecular hardness is a measure of molecular stability. It can be found that larger hardness and smaller log *P* values for title complex than chloroquine molecule. So, molecular hardness is inversely proportional to biological activity.

3.11. NBO analysis.

The Natural Bond Orbital (NBO) analysis of the antimalarial drug of chromium arene–quinoline half sandwich complex has illustrated the character of electronic conjugation between the bonds in this drug.

3.11.1. Charge distribution.

Figure 5 indicates a bar diagram representing the charge distribution in title drugs from the natural population analysis (NPA). The largest negative charges (-0.67 e) are placed on the N atom of the amino group.

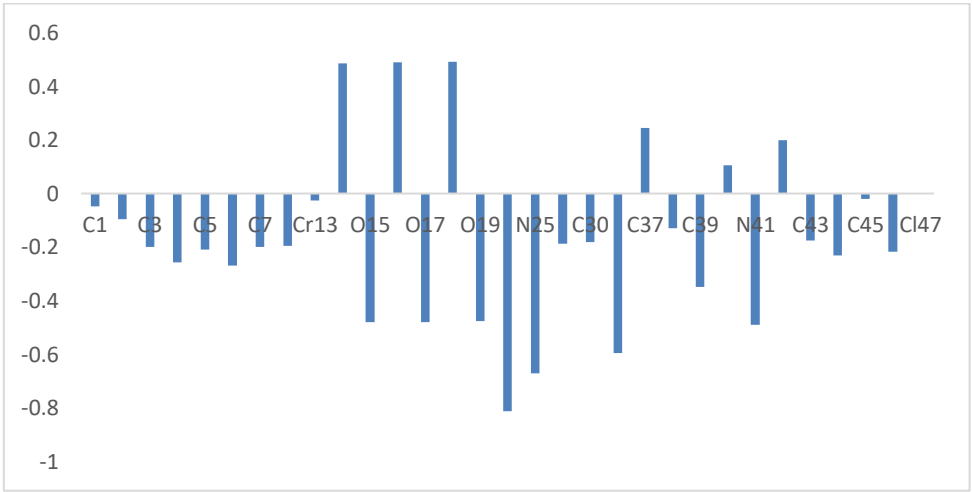

Figure 5. Bar diagram representing the charge distribution in title complex from the natural population analysis (NPA).

The calculated natural charge of Cr atom is -0.026 e. this value is noticeably smaller than the formal charge of +1. This is an outcome of noteworthy charge donation from the ligands.

According to the NBO results, the electron configuration of Cr is:

$$[core]4s^{0.01}\ 3d^{5.60}\ 4p^{0.08}\ 5s^{0.36}\ 4d^{0.01}$$

The natural population of core, valence and 0.45 Rydberg are 17.97, 6.03, and 0.02, respectively. Therefore, the total natural population on the Cr is 24.026. This is compatible with the calculated natural charge in the Cr atom in the title drug -0.026 e, which matches the difference between 24.026 e and the total number of electrons in the isolated Cr atom (24 e).

3.11.2. Character of natural hybrid orbital (NHO).

The Cr-CO bonds of the title complex are formed by the interaction between sp^md^n orbital centered on the Cr ion and an $sp^{0.55}$ orbital on the carbon atom of the carbonyl ligand. The occupancies of the electrons and polarization coefficients in these bonds are listed in Table 3. It can be deduced a higher polarization through the carbon atom. This indicates a strong polarization directed toward the C atom.

Table 3. Occupancies of the electrons and polarization coefficients in the Cr-CO bonds of title complex at mPW1PW91/6-311G(d,p) level of theory**.**

Bond orbital	Occupancy	Hybrids
BD (1)Cr - C 14	1.95901	$0.5526\ (sp^{0.14}d^{3.97})_{Cr} + 0.8335\ (sp^{0.55})_C$
BD (1)Cr - C 16	1.96122	$0.5545\ (sp^{0.14}d^{4.04})_{Cr} + 0.8322\ (sp^{0.55})_C$
BD (1)Cr - C 18	1.96014	$0.5490\ (sp^{0.13}d^{3.83})_{Cr} + 0.8358\ (sp^{0.55})_C$

3.12. Quantum Theory of Atoms in Molecules (QTAIM) analysis.

QTAIM analysis has been provided to explore the studied drug's physical and chemical characterizations of the Cr-C bonds. The calculated electron density values at critical bond points (ρ_{BCP}) of the Cr-CO bond is 0.1357 a.u. Laplacian electron density of critical bond points ($\nabla^2\rho$) of Cr-CO bond is 0.4926. These positive values at the corresponding BCP reveal that closed-shell interactions can be expected in the Cr-CO bonds. The total electron energy density (H) value of BCP(Cr-O) is -0.0550 a.u. This negative value is an indicator of covalency. The $\nabla^2\rho>0$ values and $H<0$ values of Cr-CO bonds are well-matched with like outcomes for the M-C bonds in organometallic complexes [66-68]. These values reveal a combination of the closed-shell and shared interactions for the metal-ligand bonds.

4. Conclusions

Quantum chemical calculations in an antimalarial drug of chromium arene–quinoline half sandwich complex in gas and aqueous phases revealed the hardness and electrophilicity values of the complex were smaller in the gas phase than aqueous medium. But, the complex's chemical potential value increased from the gas phase to the aqueous medium. It has longer Cr-C and shorter bond distances in the aqueous phase compared to the gas phase. These variations may change the biological activities of the drugs. Molecular hardness indicated an inverse relation to biological activity. The most intense vibrational bands belonged to CO ligands' symmetric and asymmetric strength vibrations. The corresponding calculated wavenumber values were smaller in the aqueous phase than in the gas phase. The calculated log P value of the title complex was less than chloroquine. NBO calculations indicated that Cr-

CO bonds of the title complex were formed by the interaction between sp^md^n orbital centered on the Cr ion and an $sp^{0.55}$ orbital on the carbon atom of the carbonyl ligand. QTAIM results show that Cr-CO bonds are a mixture of shared and closed-shell interactions.

Funding

This research did not receive any specific funding.

Acknowledgment

Declared none.

Conflicts of Interest

The authors declare they have no conflict of interest.

References

1. Talisuna, A.O.; Bloland, P.; D'Alessandro, U.D. History, Dynamics, and Public Health Importance of Malaria Parasite Resistance. *Clin. Microbiol. Rev.* **2004**, *17*, 235-254, https://doi.org/10.1128/CMR.17.1.235-254.2004.
2. Mita, T.; Tanabe, K.; Kita, K. Spread and evolution of *Plasmodium falciparum* drug resistance. *Parasitol. Int.* **2009**, *58*, 201-209, https://doi.org/10.1016/j.parint.2009.04.004.
3. Aronimo, B.S.; Okoro, U.C.; Ali, R.; Ibeji, C.U.; Ezugwu, J.A.; Ugwu, D.I. Synthesis, molecular docking and antimalarial activity of phenylalanine-glycine dipeptide bearing sulphonamide moiety. *Journal of Molecular Structure* **2021**, *1246*, 131201, https://doi.org/10.1016/j.molstruc.2021.131201.
4. Savir, S.; Liew, J.W.K.; Vythilingam, I.; Lim, Y.A.L.; Tan, C.H.; Sim, K.S.; Lee, V.S.; Maah, M.J.; Tan, K.W. Nickel(II) Complexes with Polyhydroxybenzaldehyde and O,N,S tridentate Thiosemicarbazone ligands: Synthesis, Cytotoxicity, Antimalarial Activity, and Molecular Docking Studies. *Journal of Molecular Structure* **2021**, *1242*, 130815, https://doi.org/10.1016/j.molstruc.2021.130815.
5. Pashynska, V.; Stepanian, S.; Gömöry, Á.; Adamowicz, L. What are molecular effects of co-administering vitamin C with artemisinin-type antimalarials? A model mass spectrometry and quantum chemical study. *Journal of Molecular Structure* **2021**, *1232*, 130039, https://doi.org/10.1016/j.molstruc.2021.130039.
6. Benjamin, I.; Udoikono, A.D.; Louis, H.; Agwamba, E.C.; Unimuke, T.O.; Owen, A.E.; Adeyinka, S.A. Antimalarial potential of naphthalene-sulfonic acid derivatives: Molecular electronic properties, vibrational assignments, and in-silico molecular docking studies. *Journal of Molecular Structure* **2022**, *1264*, 133298, https://doi.org/10.1016/j.molstruc.2022.133298.
7. Salituro, L.J.; Pazienza, E.; Rychnovsky, S.D. Total Syntheses of Strasseriolide A and B, Antimalarial Macrolide Natural Products. *Organic Letters* **2022**, *24*, 1190-1194, https://doi.org/10.1021/acs.orglett.1c04340.
8. Hernandes, I.S.; Da Silva, H.C.; Dos Santos, H.F.; De Almeida, W.B. Unveiling the Molecular Structure of Antimalarial Drugs Chloroquine and Hydroxychloroquine in Solution through Analysis of ^{1}H NMR Chemical Shifts. *The Journal of Physical Chemistry B* **2021**, *125*, 3321-3342, https://doi.org/10.1021/acs.jpcb.1c00609.
9. Li, S.; Xu, W.; Wang, H.; Tang, T. et al. Ferroptosis plays an essential role in the antimalarial mechanism of low-dose dihydroartemisinin. *Biomedicine & Pharmacotherapy* **2022**, *148*, 112742, https://doi.org/10.1016/j.biopha.2022.112742.
10. Anwar, S.; DasGupta, D.; Azum, N.; Alfaifi, S.Y.M.; Asiri, A.M.; Alhumaydhi, F.A.; Alsagaby, S.; Sharaf, S.; Shahwan, M.; Hassan, M.I. Inhibition of PDK3 by artemisinin, a repurposed antimalarial drug in cancer therapy. *Journal of Molecular Liquids* **2022**, *355*, 118928, https://doi.org/10.1016/j.molliq.2022.118928.
11. Kant, R.; Yadav, P.; Singh, M.; Meena, M.K. Challenges with the proposed approach in enhancing the accessibility of antimalarial activities during COVID 19 pandemic. *Journal of Infection and Public Health* **2021**, *14*, 1089-1094, https://doi.org/10.1016/j.jiph.2021.06.015.

12. Dillarda, L.K.; Fullerton, A.M.; McMahon, C.M. Ototoxic hearing loss from antimalarials: A systematic narrative review. *Travel Medicine and Infectious Disease* **2021**, *43*, 102117, https://doi.org/10.1016/j.tmaid.2021.102117.
13. Van de Walle, T.; Cools, L.; Mangelinckx, S.; D'hooghe, M. Recent contributions of quinolines to antimalarial and anticancer drug discovery research. *European Journal of Medicinal Chemistry* **2021**, *226*, 113865, https://doi.org/10.1016/j.ejmech.2021.113865.
14. Hastings, I.M.; Bray, P.G.; Ward, S.A. A requiem for chloroquine. *Science* **2002**, *298*, 74–75, https://doi.org/10.1126/science.1077573.
15. Beagley, P.; Blackie, M.A.; Chibale, K.; Clarkson, C.; Moss, R.; Smith, P.J. Synthesis and antimalarial activity *in vitro* of new ruthenocene–chloroquine analogues. *J. Chem. Soc., Dalton Trans* **2002**, 4426–4433, https://doi.org/10.1039/B205432A.
16. Atteke, C.; Ndong, J.M.M.; Aubouy, A.; Maciejewski, L.A.; Brocard, J.; Lebibi, J.; Deloron, P. In vitro susceptibility to a new antimalarial organometallic analogue, ferroquine, of Plasmodium falciparum isolates from the Haut-Ogooué region of Gabon. *J. Antimicrob. Chemother.* **2003**, *51*, 1021-1024, https://doi.org/10.1093/jac/dkg161.
17. Biot, C.; Delhaes, L.; Abessolo, H. et al. Novel metallocenic compounds as antimalarial agents. Study of the position of ferrocene in chloroquine. *J. Organomet. Chem.* **1999**, *589*, 59-65, https://doi.org/10.1016/S0022-328X(99)00302-2.
18. Biot, C. Ferroquine: A New Weapon in the Fight Against Malaria. *Curr. Med. Chem.: Anti-infect. Agents* **2004**, *3*, 135-147, https://doi.org/10.2174/1568012043354008.
19. http://clinicaltrials.gov/ct2/show/NCT00988507, accessed 02.02.2011.
20. Hubel, R.; Polborn, K.; Knizek, J.; Nöth, H.; Beck, W. Palladium(II)- und Platin(II)-Komplexe mit dem Antimalariamittel Mefloquin als Liganden. *Z. Anorg. Allg. Chem.* **2000**, *626*, 1701-1708, https://doi.org/10.1002/1521-3749(200007)626:7%3C1701::AID-ZAAC1701%3E3.0.CO;2-J.
21. Navarro, M.; Vasquez, F.; Sanchez-Delgado, R.A.; Perez, H.; Sinou, V.; Schrevel, J. Toward a Novel Metal-Based Chemotherapy against Tropical Diseases. 7. Synthesis and in Vitro Antimalarial Activity of New Gold−Chloroquine Complexes. *J. Med. Chem.* **2004**, *47*, 5204-5209, https://doi.org/10.1021/jm049792o.
22. Ocheskey, J.A.; Harpstrite, S.E.; Oksman, A.; Goldberg, D.E.; Sharma, V. Metalloantimalarials: synthesis and characterization of a novel agent possessing activity against *Plasmodium falciparum*. *Chem. Commun* **2005**, 1622-1624, https://doi.org/10.1039/B415771K.
23. Dubar, F.; Bohic, S.; Dive, D.; Guerardel, Y.; Cloetens, P.; Khalife, J.; Biot, C. Deciphering the Resistance-Counteracting Functions of Ferroquine in Plasmodium falciparum-Infected Erythrocytes. *ACS Med. Chem. Lett.* **2012**, *3*, 480–483, https://doi.org/10.1021/ml300062q.
24. Biot, C.; Glorian, G.; Maciejewski, L.A.; Brocard, J.S.; Domarle, O.; Blampain, G.; Millet, P.; Georges, A.J.; Lebibi, J. Synthesis and Antimalarial Activity in Vitro and in Vivo of a New Ferrocene−Chloroquine Analogue. *J. Med. Chem.* **1997**, *40*, 3715-3718, https://doi.org/10.1021/jm970401y.
25. Biot, C.; Daher, W.; Ndiaye, C.M. et al. Probing the Role of the Covalent Linkage of Ferrocene into a Chloroquine Template. *J. Med. Chem.* **2006**, *49*, 4707–4714, https://doi.org/10.1021/jm060259d.
26. Biot, C.; Daher, W.; Chavain, N.; Fandeur, T.; Khalife, J.; Dive, D.; Clercq, E.D. Design and Synthesis of Hydroxyferroquine Derivatives with Antimalarial and Antiviral Activities. *J. Med. Chem.* **2006**, *49*, 2845–2849, https://doi.org/10.1021/jm0601856.
27. Xiao, J.; Sun, Z.; Kong, F.; Gao, F.,.Current scenario of ferrocene-containing hybrids for antimalarial activity.*Eur. J. Med. Chem.*. **2020** *185*, 111791, https://doi.org/ 10.1016/j.ejmech.2019.111791.
28. Glans, L.; Taylor, D.; de Kock, C.; Smith, P.J.; Haukka, M.; Moss, J.R.; Nordlander, E. Synthesis, characterization and antimalarial activity of new chromium arene–quinoline half sandwich complexes. *Journal of Inorganic Biochemistry* **2011**, *105*, 985–990, https://doi.org/10.1016/j.jinorgbio.2011.03.019.
29. Ghiasi, R.; Sofiyani, M.V.; Emami, R. Computational investigation of interaction of titanocene dichloride anti-cancer drug with carbon nanotube in presence of external electric field. *Biointerface Research in Applied Chemistry* **2021**, *11*, 12454 - 12461, https://doi.org/10.33263/BRIAC114.1245412461.
30. Kazemi, Z.; Ghiasi, R.; Jamehbozorgi, S. The interaction of 5-fluorouracil with graphene in presence of external electric field: A theoretical investigation. *Adsorption* **2020**, *26*, 905–911, https://doi.org/10.1007/s10450-019-00140-3.
31. Norouzi, P.; Ghiasi, R. Theoretical Understanding the Effects of External Electric Field on the Hydrolysis of anticancer drug titanocene dichloride. *Molecular Physics* **2020**, *118*, e1781272, https://doi.org/10.1080/00268976.2020.1781272.

32. Norouzi, P.; Ghiasi, R.; Fazaeli, R. Effects of External Electric Field on the Hydrolysis of Cisplatin: A Density Functional Theory Approach. *Russian Journal of Inorganic Chemistry* **2020**, *65*, 2053–2061, https://doi.org/10.1134/S0036023620140041.
33. Rezazadeh, M.; Ghiasi, R.; Jamehbozorgi, S. Solvent Effects on the Structure And Spectroscopic Properties of the Second-Generation Anticancer Drug Carboplatin: A Theoretical Insight. *Journal of Structural Chemistry* **2018**, *59*, 245-251, https://doi.org/10.1134/S0022476618010390.
34. Rezazadeh, M.; Ghiasi, R.; Jamehbozorgi, S. Influence of Solvent and Electric Field on the Structure and IR,31P NMR Spectroscopic Properties of a Titanocene–Benzyne Complex. *Journal of Applied Spectroscopy* **2018**, *85*, 526-534, https://doi.org/10.1007/s10812-018-0683-8.
35. Shabani, M.; Ghiasi, R.; Zare, K.; Fazaeli, R. The Interaction between carboplatin anticancer drug and $B_{12}N_{12}$ nano-cluster: A computational investigation *Main Group Chemistry* **2021**, *20*, 345–354.
36. Shabani, M.; Ghiasi, R.; Zare, K.; Fazaeli, R. Computational investigation of interaction between titanocene dichloride and nanoclusters ($B_{12}N_{12}$, $B_{12}P_{12}$, $Al_{12}N_{12}$ and $Al_{12}P_{12}$). *Main Group Chemistry* **2021**, *20*, 437-446, https://doi.org/10.3233/mgc-210010.
37. Ghiasi, R.; Rahimi, M. Complex formation of Titanocene Dichloride Anticancer and $Al_{12}N_{12}$ Nano-cluster: A Quantum Chemical Investigation of Solvent, Temperature and Pressure Effects. *Main Group Chemistry* **2021**, *20*, 19–32, http://doi.org/10.3233/mgc-210034.
38. Ghiasi, R.; Emami, R.; Sofiyani, M.V. Interaction between carboplatin with $B_{12}P_{12}$ and $Al_{12}P_{12}$ nano-clusters: A computational investigation *Phosphorus, Sulfur, and Silicon and the Related Elements* **2021**, *196*, 751–759, https://doi.org/10.1080/10426507.2021.1920590.
39. Kazemi, Z.; Ghiasi, R.; Jamehbozorgi, S. Analysis of the Interaction Between the C_{20} Cage and cis-$PtCl_2(NH_3)_2$: A DFT Investigation of the Solvent Effect, Structures, Properties, and Topologies. *Journal of Structural Chemistry* **2018**, *59*, 1044-1051, https://doi.org/10.1134/S0022476618050050.
40. Frisch, M.J.; Trucks, G.W.; Schlegel, H.B. et al. *Gaussian 09* **2009,** Revision A.02, Gaussian Inc., Wallingford CT.
41. Hay, P.J. Gaussian basis sets for molecular calculations. The representation of *3d* orbitals in transition-metal atoms. *J. Chem. Phys.* **1977**, *66*, 4377, https://doi.org/10.1063/1.433731.
42. Krishnan, R.; Binkley, J.S.; Seeger, R.; Pople, J.A. Self-consistent molecular orbital methods. XX. A basis set for correlated wave functions. *J. Chem. Phys.* **1980**, *72*, 650, https://doi.org/10.1063/1.438955.
43. McLean, A.D.; Chandler, G.S. Contracted Gaussian-basis sets for molecular calculations. 1. 2nd row atoms, Z=11-18. *J. Chem. Phys.* **1980**, *72*, 5639, https://doi.org/10.1063/1.438980.
44. Wachters, A.J.H. Gaussian basis set for molecular wavefunctions containing third-row atoms. *J. Chem. Phys.* **1970**, *52*, 1033, https://doi.org/10.1063/1.1673095.
45. Adamo, C.; Barone, V. Exchange functionals with improved long-range behavior and adiabatic connection methods without adjustable parameters: The *m*PW and mPW1PW models. *J. Chem. Phys.* **1998**, *108*, 664, https://doi.org/10.1063/1.475428.
46. Dunbar, R.C. Metal Cation Binding to Phenol: DFT Comparison of the Competing Sites. *J. Phys. Chem. A* **2002**, *106*, 7328-7337, https://doi.org/10.1021/jp013588k.
47. Porembski, M.; Weisshaar, J.C. Kinetics and Mechanism of the Reactions of Ground-State Y ($4d^15s^2$, ^2D) with Ethylene and Propylene: Experiment and Theory. *J. Phys. Chem. A* **2001**, *105*, 6655-6667, https://doi.org/10.1021/jp010646t.
48. Porembski, M.; Weisshaar, J.C. Singlet and Triplet Reaction Paths for Gas-Phase Zr + C_2H_4 by Density Functional Theory. *J. Phys. Chem. A* **2001**, *105*, 4851-4864, https://doi.org/10.1021/jp010219f.
49. Porembski, M., Weisshaar, J. C.; Singlet and Triplet Reaction Paths for Gas-Phase Zr + C_2H_4 by Density Functional Theory. *J. Am. Chem. Soc.* **2001**, *105*, 4851–4864, https://doi.org/10.1021/jp010219f.
50. Tomasi, J.; Mennucci, B.; Cammi, R. Quantum mechanical continuum solvation models. *Chem. Rev.* **2005**, *105*, 2999-3094, https://doi.org/10.1021/cr9904009.
51. Kim, T.; Park, H. Computational prediction of octanol–water partition coefcient based on the extended solvent-contact model. *J. Mol. Graph. Model* **2015**, *60*, 108–117, https://doi.org/10.1016/j.jmgm.2015.06.004.
52. Reed, A.E.; Curtiss, L.A.; Weinhold, F. Intermolecular interactions from a natural bond orbital, donor-acceptor viewpoint. *Chem. Rev.* **1988**, *88*, 899-926, https://doi.org/10.1021/cr00088a005.
53. Glendening, E.D.; Reed, A.E.; Carpenter, J.E.; Weinhold, F. *NBO Version 3.1* **2003**, Gaussian Inc., Pittsburgh.

54. Lu, T.; Chen, F. Multiwfn: A Multifunctional Wavefunction Analyzer. *J. Comp. Chem.* **2012**, *33*, 580-592, https://doi.org/10.1002/jcc.22885.
55. Lu, T.; Chen, F. Quantitative analysis of molecular surface based on improved Marching Tetrahedra algoritm. *J. Mol. Graph. Model* **2012**, *38*, 314-323, https://doi.org/10.1016/j.jmgm.2012.07.004.
56. Kassimi, N.E.-B.; Doerksen, R.J.; Thakkar, A.J. Polarizabilities of Aromatic Five-Membered Rings: Azoles. *J. Phys. Chem.* **1995**, *99*, 12790–12796, https://doi.org/10.1021/j100034a017.
57. Chattaraj, P.K.; Nath, S.; Maiti, B. *Reactivity descriptors. In: Tollenaere, J.; Bultinck, P.; Winter, H.D.; Lengeneaker, W. (Eds.) Computational Medicinal Chemistry for Drug Discovery* **2003**, CRC Press, Boca Raton, https://doi.org/10.1201/9780203913390.
58. Verma, R.P.; Hansch, C. A comparison between two polarizability parameters in chemical–biological interactions. *Bioorg. Med. Chem.* **2005**, *13*, 2355-2372, https://doi.org/10.1016/j.bmc.2005.01.051.
59. Verma, R.P.; Kurup, A.; Hansch, C. On the role of polarizability in QSAR. *Bioorg. Med. Chem.* **2005**, *13*, 237-255, https://doi.org/10.1016/j.bmc.2004.09.039.
60. Fleming, I. *Molecular Orbitals and Organic Chemical Reactions* **1976**. John Wiley & Sons, London.
61. Geerlings, P.; De Proft, F.; Langenaeker, W. Conceptual Density Functional Theory. *Chemical Reviews* **2003**, *103*, 1793-1874, https://doi.org/10.1021/cr990029p.
62. Parr, R.G.; Pearson, R.G. Absolute hardness: companion parameter to absolute electronegativity. *Journal of the American Chemical Society* **1983**, *105*, 7512-7516, https://doi.org/10.1021/ja00364a005.
63. Parr, R.G.; Szentpály, L.v.; Liu, S. Electrophilicity Index. *Journal of the American Chemical Society* **1999**, *121*, 1922-1924, https://doi.org/10.1021/ja983494x.
64. Flippin, L.A.; Gallagher, D.W.; Jalali-Araghi, K. A convenient method for the reduction of ozonides to alcohols with borane-dimethyl sulfide complex. *The Journal of Organic Chemistry* **1989**, *54*, 1430-1432, https://doi.org/10.1021/jo00267a035.
65. Ott, B.; Boerio-Goates, J. *Chemical Thermodynamics: Principles and Applications* **2000**. Elsevier-Academic Press, https://doi.org/10.1016/B978-0-12-530990-5.X5000-7.
66. Saraf, S.H.; Ghiasi, R. Quantum theory of atoms in molecules, electron localization function, and localized-orbital locator investigations on *trans*-(NHC)PtI_2(*para*-NC_5H_4X) complexes. *Journal of Chemical Research* **2020**, *44*, 482–486, https://doi.org/10.1177%2F1747519820907243.
67. Zafarniya, F.; Ghiasi, R.; Jameh-Bozorgi, S. Solvent effect on the linkage isomerism in $[Fe(CO)_4(NCS)]^-$ and $[Fe(CO)_4(SCN)]^-$anions: A theoretical investigation. *Physics and Chemistry of Liquids* **2017**, *55*, 444-456, https://doi.org/10.1080/00319104.2016.1218877.
68. Zafarnia, F.; Ghiasi, R.; Jamehbozorgi, S. Computational study of osmabenzyne: The solvent effects on the structure and spectroscopic properties (IR, NMR). *Journal of Structural Chemistry* **2017**, *58*, 1324-1331, https://doi.org/10.1134/S0022476617070083.